2020 IEEE International Conference on Robotics and Automation (ICRA)
31 May - 31 August, 2020. Paris, France

Human Interface for Teleoperated Object Manipulation with a Soft Growing Robot

Fabio Stroppa, Ming Luo, Kyle Yoshida, Margaret M. Coad,
Laura H. Blumenschein, and Allison M. Okamura

***Abstract*— Soft growing robots are proposed for use in applications such as complex manipulation tasks or navigation in disaster scenarios. Safe interaction and ease of production promote the usage of this technology, but soft robots can be challenging to teleoperate due to their unique degrees of freedom. In this paper, we propose a human-centered interface that allows users to teleoperate a soft growing robot for manipulation tasks using arm movements. A study was conducted to assess the intuitiveness of the interface and the performance of our soft robot, involving a pick-and-place manipulation task. The results show that users were able to complete the task 97% of the time and achieve placement errors below 2 cm on average. These results demonstrate that our body-movement-based interface is an effective method for control of a soft growing robot manipulator.**

I. INTRODUCTION

Soft and continuum robots have useful features that are advantageous in applications requiring delicate interaction, e.g. object manipulation [1]–[3], or adaptation to unknown environments, e.g. navigation and exploration [4], [5]. A subset of soft and continuum robots have an additional feature that makes operation in confined environments easier: the ability to extend or grow as an additional degree of freedom [4]–[7]. By extending and shortening in length, these systems can move their tip through cluttered environments without being restricted by body parts that may collide with obstacles, such as the "elbows" on a typical rigid serial-chain robot arm. For this reason, growth can be especially beneficial in manipulation tasks.

While the growth degree of freedom has benefits in cluttered environments, designing control to leverage those benefits is challenging. In general, there do not exist well-defined kinematic models for soft robots, so often control of soft robots happens in joint space instead of task space [8]. Even when approximate kinematic models exist, the output shape or behavior of the robot can be difficult to measure, and therefore hard to close a loop around. Thus, one strategy to control soft robotic systems is to use the human to close the loop on position and account for errors caused by inaccurate models and lack of sensing and closed-loop control. However, dissimilarity between the degrees of freedom of the robot and the human makes it difficult to find appropriate control interfaces.

Toyota Research Institute (TRI) provided funds to assist the authors with their research but this article solely reflects the opinions and conclusions of its authors and not TRI or any other Toyota entity.

The authors are with the Mechanical Engineering Department, Stanford University, Stanford, CA 94305, USA fstroppa@stanford.edu

Fig. 1. An operator controlling the soft growing robot with the gesture-based Body Interface. Here the operator is shown physically near the robot, which is safe due to the robot's low inertia and soft exterior, while in our experimental study the operators controlled the robot from a slightly farther distance.

Studies have used devices such as 3D mice [9], joysticks and gamepads for gaming [9]–[11], haptic interfaces [9], [12], rigid-link manipulators [13], and even flexible joysticks specially designed for soft robots [14]. In particular, the work of El-Hussieny et al. [14] was specifically designed for soft growing robots and proved to be intuitive and easy to use. However, all these interfaces rely on physical devices, which may not be the most intuitive way for humans to control (and learn to control) the robot. Here we remove the physical interface and use the human body to control the robot.

In this work, we propose an interface that allows human operators to control the robot simply by using their arm. The gestures of the operator, tracked by a motion capture system, are mapped to the kinematics of the robot for an easy and intuitive teleoperation. This interface, called the "Body Interface" (Fig. 1), was used in an experimental study to assess its effectiveness in the control of a soft growing robot in a teleoperated manipulation task. Twelve participants were able to successfully teleoperate the robot to reach, grasp, and move objects in the workspace.

The rest of the paper is organized as follows: Sec. II discusses the interface, Sec. III describes the design and control of the soft growing robot, Sec. IV discusses the experiment setup and results, and, finally, Sec. V summarizes the work and presents possible future research.

II. BODY INTERFACE

The interface for teleoperating the robot, the Body Interface, is based on a Motion Capture Tracking system and a

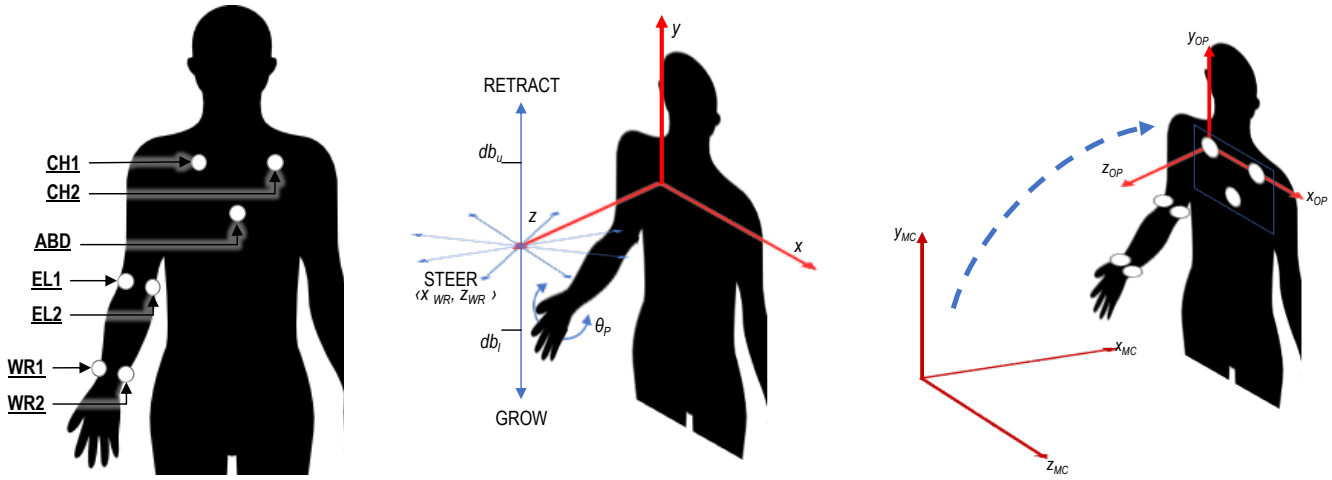

(a) (b) (c)

Fig. 2. (a) Motion capture marker layout on the operator's upper body. (b) Commands used to control the robot based on direction of movement. (c) The original reference system is transformed to be aligned with the plane where the markers *CH1*, *CH2*, and *ABD* lie, with origin at *CH1*.

Gesture Interpreter Tool. The interface tracks the operator's gestures, maps them to the kinematics of the robot, and sends the commands.

A. Motion Capture Tracking

We used the *PhaseSpace Impulse X2E* (phasespace.com) system to track the operator's movements. This accurate optical tracking mechanism was used in order to test the effectiveness of the interface while avoiding the performance limitations of other types of sensors. In practice, other tracking systems could be employed.

Our motion capture setup includes six lightweight-linear-detector cameras monitoring seven active LED markers placed on the forearm and the chest of the operator. The gestures are tracked in real time at 270 Hz. As shown in Fig. 2(a), the Body Interface exploits four markers on the operator's forearm for gesture recognition (two on the elbow *EL1* and *EL2*, two on the wrist *WR1* and *WR2*), and three on the operator's chest to create a body centered reference system (*CH1*, *CH2*, and *ABD*).

B. Gesture Interpreter Tool

The operator's gestures are mapped to the kinematics of the robot through our custom Gesture Interpreter Tool (GIT). The GIT recognizes three types of commands: grow/retract, steer left/right/backwards/forwards, and rotate the end effector. One command of each type can be given simultaneously. The communication with the robot's microcontroller is realized via a serial port at 66 Hz.

The specific mapping between the gestures and commands can be customized based on the application. Fig. 2(b) shows one proposed mapping, used to control a soft robot hanging from the ceiling and growing in the direction of gravity. Moving the forearm above and below the operator's transverse plane (forearm flexion/extension) will make the robot retract and grow, respectively; whereas all the movements parallel to the transverse plane are mapped as steering movements (forearm back and forth and medial/lateral rotation, respectively backwards/forwards and left/right); finally, pronosupination defines the end effector rotation.

1) Calibration and Command Mapping: The location of the wrist defines the sent commands. Since the interface is based on body movements, the system needs an initial calibration to account for the operator's reach workspace.

The steering commands are mapped to the x and z coordinates of the wrist. The wrist location *WR* (the centroid of *WR1* and *WR2*) is projected to the operator's transverse plane to give the coordinates $\langle x_{WR}, z_{WR} \rangle$. During the calibration, the system stores the limits of the operator's reach in the four directions (left/right/backwards/forwards), which will then correspond to the limits of the robot's workspace.

The command of growth/retraction is triggered when the operator's hand exceeds a certain threshold of y_{WR}. During calibration, the operator defines a deadband ($[db_l, db_u]$) along the y axis: if the y coordinate of *WR* falls within this region, the robot keeps its length fixed; otherwise, it grows or retracts at a fixed speed, based on the position of the operator's hand. In this case, the calibration of the deadband is defined by half of the operator's reachable limits, to allow the operator to easily steer and change length simultaneously.

Finally, the angle θ_P defines the rotation of the end effector. This is the angle between the two segments $WR1-WR2$ and $EL1-EL2$ when their projection lies on the operator's coronal plane. During calibration, the offset between θ_P and the starting orientation of the end effector is stored to assure the operator's comfort during the teleoperation.

2) Reference System Alignment: In order to properly retrieve the data, the GIT needs to define a body centered reference system. The three chest markers allow the operator to be aligned to the motion capture reference system, resulting in an interface that is independent of the operator's

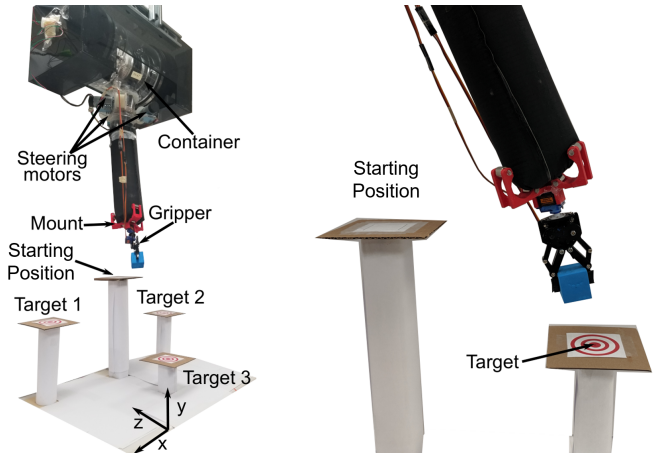

Fig. 3. (a) The soft growing robot with its components, and the proposed task scenario with the orientation of the operator's reference system. (b) The soft robot during the manipulation task, moving a block to a specific target.

pose in space. As shown in Fig. 2(c), the frame defined by the calibration of the Motion Capture system $\langle x_{MC}, y_{MC}, z_{MC}\rangle$ is transformed into the reference system of the operator $\langle x_{OP}, y_{OP}, z_{OP}\rangle$, such that the coordinates of the markers are expressed with reference to the latter. In particular, *CH1*, *CH2*, and *ABD* define a plane, which the GIT transforms to be lying on the x_{OP}-y_{OP} plane, with *CH1* placed at the origin of the new reference system. The operator can therefore control the robot in whatever body pose is most comfortable.

III. SOFT-GROWING ROBOT

We built a soft growing robot specifically for manipulation tasks. This section describes its design and control strategies.

A. Design

The soft growing manipulator can grow, retract, and steer in three dimensions while carrying a payload, as shown in Fig. 3. The device grows and retracts from a portable, sealed container. The soft growing manipulator everts, adding new material at the tip, when pressurized, and the DC motor inside the container pulls at the tip to invert the material for retraction. The details of the fabrication of the soft growing manipulator and the design of the manipulator's container are described in [4]. The robot is made of a heat-sealable thermoplastic polyurethane fabric sheet and can grow to up to 1.5 m, with a diameter of 10 cm. Unlike in [4], the continuum robot is steered using a a cable-driven system. The steering system consists of three cables evenly spaced around the robot circumference, driven by three gearmotors mounted at the robot container (*Pololu 131:1 37DX73LM*). To steer, the cables shorten, causing the robot to bend in the direction of the cable. A gripper is positioned at the distal end of the manipulator. The gripper is driven by two servo motors, one for rotation and the other for grasping. The gripper (*Standard Gripper Kit-Rollpaw, SunFounder*) connects to and moves along the tip of the robot with a magnetic attachment based off the one presented in [15], allowing for the completion of grasping and manipulation tasks.

B. Control

With reference to the parameters described in Sec. II, the Body Interface controls the following robot parameters:

- the end effector position (in meters), given by $\langle x_{WR}, z_{WR}\rangle$, these are the two coordinates of the tip of the robot given a certain length of the body[1];
- the orientation of the gripper (in radians), given by the angle θ_P; and
- the direction of length change, either growing, retracting, or static, given by y_{WR} relative to the growth deadband $[db_l, db_u]$. When the deadband is exceeded, the robot is commanded to grow or retract at a constant rate (in radians per second)[2].

Because the robot tip does not have tracking sensors, the controller relies on the human operator to close the loop and achieve the desired end effector position. Control strategies match with what is generally used for continuum robots, and are based on the constant curvature model [16]; more details can be found in our previous work [4]

For the experiment described in Section IV, the operator opens and closes the gripper with a verbal command to the investigator.

IV. EXPERIMENTAL STUDY

The Body Interface was tested on a pick-and-place task to evaluate its usability in terms of accuracy, timing, and workload.

A. Participants

Twelve participants took part in the experiment (seven males, 26 ± 3 yrs old; and five females, 22 ± 3 yrs old). All participants were right handed and had no known impairment affecting their upper limb. The protocol was approved by the Stanford University Institutional Review Board, and written informed consent was obtained from each participant.

B. Task and Scenario

Figures 1 and 3 show the scenario of the experiment. The participants were asked to pick up a block placed on a starting pillar underneath the robot's base and then move the block onto a designated target. There were three targets placed over three different pillars, and all the participants repeated the task five times for each target, for a total of fifteen repetitions. The experiment was designed such that the participants were randomly and equally divided to explore all the six combinations of target ordering.

The setup details are as follows:

- the *Block*, size 3.4×3.4 cm, placed at the center of the workspace on a pillar 30 cm tall;

[1]The coordinate along the direction of growth may vary when the length of the robot is fixed, as a result of steering.

[2]Since growth is driven by internal pressure in addition to the container motor, the actual robot growth is not constant but is upper bounded by the commanded motor speed.

- *Target 1*, placed 25 cm to the left of the block, on a pillar 20 cm tall;
- *Target 2*, placed 25 cm to the right of the block, on a pillar 17 cm tall;
- *Target 3*, placed 25 cm in front of the block, on a pillar 9 cm tall; and
- the *Robot's Base*, placed over the block, a distance of 1 m from the ground and 70 cm from the block.

The block starting location and the targets were placed in the center of support surfaces with an area of 12×12 cm, and the robot started each trial from an initial length of 50 cm measured from gripper to container. The participants were asked to face the robot as shown by the reference system in Fig. 3. This was not a necessary constraint, as the GIT fixes the reference system based on the operator's position, but it was useful to normalize the position of the participants among all the trials and assure consistency in the results.

All the participants performed the experiment after a five-minute training phase, in which they were familiarized with the robot and the interface. They were instructed to move the robot, learn how fast the commands could be performed, explore the workspace (including testing the response of small and large hand movements), and grasp the block. During the training, the investigator illustrated strategies to get a good grasp and retract without buckling the robot body.

During the experiment, a trial was considered a *failure* if the block fell to the table surface, which might be due to bad grasping, or hitting the pillar or the block itself. This most often occurred after overshooting on the growth length. Participants were asked to repeat any failed trials, such that each of them performed a total of fifteen good trials.

After the training session, the participants started the real task, changing the target every five trials based on their designed ordering. A single trial was divided into:

- *Grasping* phase, where the operator is asked to reach the block and grasp it; and
- *Placing* phase, where the operator is asked to move the block from the starting position and place it in the designed target.

These phases were executed sequentially without a break in the participant's control of the robot, and both of them involved activities such as growing towards the targets, orienting the gripper for a proper grasp, avoiding the pillars, and retracting when needed (especially after grasping the cube to avoid dragging it on the support surface). After each trial, the robot was automatically reset to its starting position and the block was manually replaced on the initial pillar by the investigator.

C. Evaluation Metrics

The task performance was evaluated based on:

- *Target Placement Error (TPE)*: the distance, measured in centimeters, between the center of block and the target once the task is finished, representing the accuracy of the placement.
- *Task Completion Time (TCT)*: the time required to complete a trial, measured in seconds. We broke this parameter into: (i) the overall time of the trial, from start to end; (ii) the time of each phase within a single trial; and (iii) the time spent performing the actual grasp or placement, excluding the time spent in reaching either the block or the target.
- *Failure Rate (FR)*: the number of trials in which the block did not reach the target, which were then repeated.
- *Standard NASA Task Load Index (NASA-TLX)*: a subjective standard assessment rating perceived workload while performing a task [17]; participants were asked questions about mental load, temporal load, effort, and frustration scale for each session, and the weighted average of these was used to calculate the overall workload.

D. Results and Discussion

Fig. 4 shows the histogram of the Target Placement Error over all trials, considering all the participants and all the targets: most of the trials resulted in errors lower than 2 cm, and in particular, three of them presented a minimum of 0.2 cm, showing that our system can achieve accurate performance in a manipulation task when operated by the Body Interface. The histogram also shows the Failure Rate: only 5 trials were discarded against 180 successful performances, which translates to a 3% FR and 97% of successful placing.

Since both the Body Interface and the robot were new to the participants at the start of the experiment, we verified if the control was intuitive enough to learn during the short training period, or if additional learning took place over the course of the trials. We plotted how performance metrics for both phases of the experiment, Grasping and Placing, changed through the 15 trials (Fig. 5). Note that Fig. 5 shows performance over time during the experiment, not organized by target, since the target order was randomized for each participant. For Grasping, we measured performance using the time it took to grasp the block. Fig. 5(a) shows the Grasping results for all participants and the average across participants, with steady performance during the experiment and only a small average improvement: this suggests that the

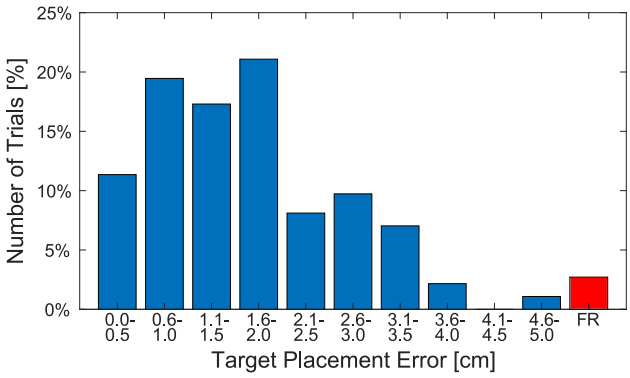

Fig. 4. Histogram of the Target Placement Error (TPE) over the all 180 trials (15 trials each for 12 participants), including all the successful block placements of the participants (in blue), compared to the number of failures that were discarded (in red).

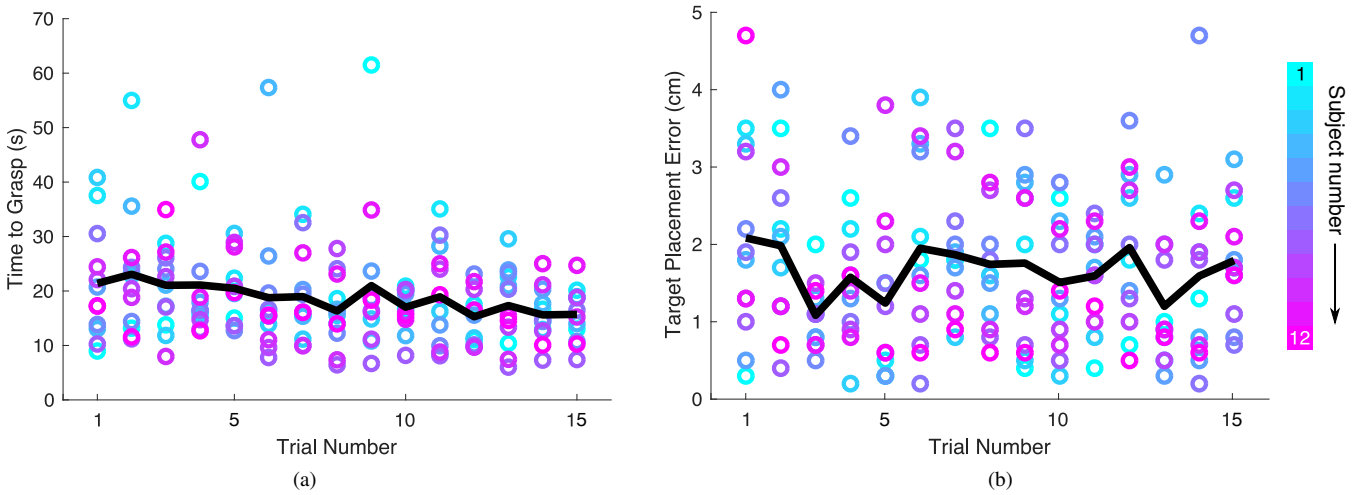

(a) (b)

Fig. 5. Performance of the manipulation task throughout the experimental study. Dots show individual participants' performance (color corresponds to participant). Average performance across participants (black line) is consistent over the experiment. (a) Grasping phase performance as measured by time to successfully grasp the object. (b) Placing phase performance as measured by Target Placement Error (TPE).

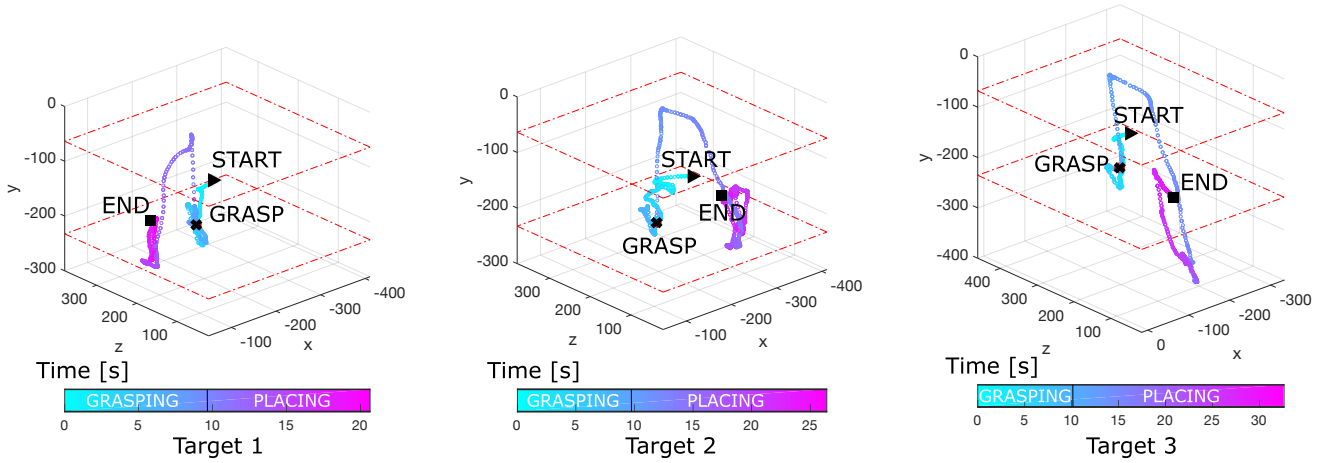

(a) (b) (c)

Fig. 6. Paths followed by the operator's hand during object manipulation trials, depicting the participant who completed the task in the shortest time for each target. Each plot indicates the starting (▶) and ending point (■), as well as the moment when the grasp was performed (✖). The planes outlined in red dashed lines represent the deadband $[db_l, db_u]$, indicating where the grow/retraction commands were triggered.

participants were able to achieve the maximum performance allowed by the dynamics of the robot.

To understand the participants' performance of the task beyond these performance metrics, we examined how participants commanded the robot to reach all three targets. Fig. 6 shows three examples of the path performed by the participants while executing the task, one for each target. Each plot illustrates the best performance in terms of timing for the respective target, and shows the path within the workspace of the participant based on the Body Interface calibration (the values of the axes are expressed in millimeters). Furthermore, the deadband $[db_l, db_u]$ is also shown to delineate where the growth and retraction commands were triggered. These plots indicate that the strategy followed by the participants was mostly consistent from target to target, and followed the instructions provided during the training phase. During the Grasping phase, participants started the trial growing towards the block, tuned the position of the gripper by steering and then performed the grasp (✖); subsequently, during the Placing phase, they retracted the robot to avoid any collision with the pillar, and then moved towards the target while steering and growing, ultimately tuning the position for the best placement. This strategy was due to the difference between the kinematics of the robot and the human arm: in particular, the sharp upwards increase in Fig. 6 does not indicate a sudden movement in the robot since the growth and retraction were rate controlled with the deadband.

We can focus on the results shown in Fig. 6 in two ways: in the breakdown in Task Completion Time, and in the location of block placement in the users' command space. As suggested by Fig. 7(a), the Placing phase took more time than the Grasping one; this is true especially for Target 3 (see also Fig. 6(c)), which was the furthest from the starting height of the cube and required more growing time. However, as shown by Fig. 7(b), if we do not consider the time spent during eversion (growth and retraction), there are no

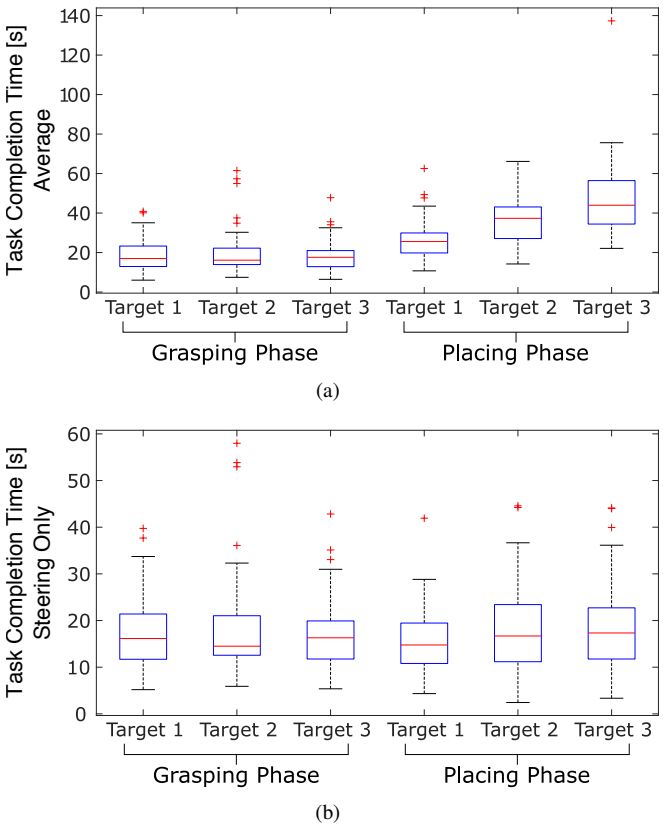

Fig. 7. Task Completion Time data for each target and each phase, including median, interquartile range with outliers, and max/min across all participants. In (a) is reported the overall time from start to end; in (b) is reported the time spent steering and tuning the final position.

noticeable differences between Grasping and Placing. This indicates that steering was equally easy at all lengths when using the Body Interface.

Looking at the locations in the command space where participants placed the block, we can see clear clusters indicating each of the three target locations (Fig. 8). The color of the dots indicate the Target Placement Error for that trial. We can see two interesting features in the data: some high error placements occurred close to the center of the clusters, and some low error placements occurred well outside. The high error dots can be explained by the quality of the grasp for that trial, since some grasps would cause the block to roll or move significantly after being released. On the other hand, even though participants were instructed to place the block on the target, the low error dots outside the clusters show where participants did not grow the robot as far and dropped the block from a height. This strategy required a larger steering command to reach the same location vertically over the target, putting those trials outside the cluster.

Lastly, the results of the NASA-TLX showed an average workload value of $68 \pm 11\%$ among all the participants, which indicates that the task was challenging but not overly demanding. The participants indicated that the Grasping phase was slightly more difficult than the Placing: it was easy to hit the block with the gripper when trying to align the robot well, especially after overshooting in growth.

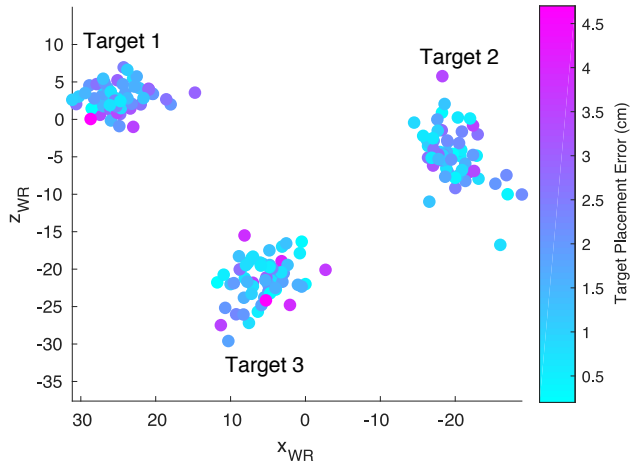

Fig. 8. Locations of placement command in users' calibrated wrist coordinates for the three targets. Color of the placement location indicates the Target Placement Error.

V. CONCLUSION

In this paper, we presented an intuitive interface to teleoperate a soft growing robot with arm gestures. We demonstrated that this interface can be used to perform a pick-and-place task by users with no previous training, achieving placement errors below 2 cm on average. This work shows a promising first step for creating interfaces that allow humans to control soft robots more intuitively and close the loop around the nonlinearities between joint and task space.

In the future, we would like to improve the performance of the soft robot for teleoperated manipulation. Specifically, the participants consistently indicated that the Grasping phase was the hardest part of the task. We believe that the primary reason is the two-finger gripper design used, and the need to align it precisely to the block surface. A possible solution is to integrate a more compliant and adaptable gripper, like a four-fingered soft gripper [18]; such a device would ensure a reliable grasp, and remove the need to accurately position the gripper in the pronosupination degree of freedom.

Another important extension of this study would be to compare the Body Interface with previous proposed control interfaces, specifically the flexible joystick proposed in [14].

Finally, the last extension of the work will be to develop shared autonomy protocols to improve the interaction during teleoperation. The results of this work have shown that, although the Body Interface can achieve good performance in terms of accuracy and timing, there is still room for improvement. By allowing the robot to participate in the execution of the task, the role of the human operator will be simplified and the different strengths of the human and the robot can be exploited. Different strategies that could be examined include: (i) haptic feedback through a holdable device [19], allowing the robot to provide guidance information to the operator and suggest the correct path to reach the targets; and (ii) artificial-intelligence algorithms mimicking the assist-as-needed paradigm used in robot-based rehabilitation [20], where the robot will move autonomously towards the target only when the operator needs help to finalize the movement and only of a limited magnitude.

REFERENCES

[1] D. Trivedi, C. D. Rahn, W. M. Kier, and I. D. Walker, "Soft robotics: Biological inspiration, state of the art, and future research," *Applied Bionics and Biomechanics*, vol. 5, no. 3, pp. 99–117, 2008.

[2] E. Brown, N. Rodenberg, J. Amend, A. Mozeika, E. Steltz, M. R. Zakin, H. Lipson, and H. M. Jaeger, "Universal robotic gripper based on the jamming of granular material," *Proceedings of the National Academy of Sciences*, vol. 107, no. 44, pp. 18 809–18 814, 2010.

[3] M. Cianchetti, T. Ranzani, G. Gerboni, T. Nanayakkara, K. Althoefer, P. Dasgupta, and A. Menciassi, "Soft robotics technologies to address shortcomings in today's minimally invasive surgery: the STIFF-FLOP approach," *Soft robotics*, vol. 1, no. 2, pp. 122–131, 2014.

[4] M. M. Coad, L. H. Blumenschein, S. Cutler, J. A. R. Zepeda, N. D. Naclerio, H. El-Hussieny, U. Mehmood, J.-H. Ryu, E. W. Hawkes, and A. M. Okamura, "Vine robots: Design, teleoperation, and deployment for navigation and exploration," *IEEE Robotics and Automation Magazine, 2019, accepted. (preprint on arXiv:1903.00069)*.

[5] M. Wooten, C. Frazelle, I. D. Walker, A. Kapadia, and J. H. Lee, "Exploration and inspection with vine-inspired continuum robots," in *IEEE International Conference on Robotics and Automation (ICRA)*, 2018, pp. 1–5.

[6] E. W. Hawkes, L. H. Blumenschein, J. D. Greer, and A. M. Okamura, "A soft robot that navigates its environment through growth," *Science Robotics*, vol. 2, no. 8, p. eaan3028, 2017.

[7] H. B. Gilbert, D. C. Rucker, and R. J. Webster III, "Concentric tube robots: The state of the art and future directions," in *Robotics Research*. Springer, 2016, pp. 253–269.

[8] D. Rus and M. T. Tolley, "Design, fabrication and control of soft robots," *Nature*, vol. 521, no. 7553, p. 467, 2015.

[9] C. Fellmann, D. Kashi, and J. Burgner-Kahrs, "Evaluation of input devices for teleoperation of concentric tube continuum robots for surgical tasks," in *Medical Imaging 2015: Image-Guided Procedures, Robotic Interventions, and Modeling*, vol. 9415. International Society for Optics and Photonics, 2015, p. 94151O.

[10] M. Csencsits, B. A. Jones, W. McMahan, V. Iyengar, and I. D. Walker, "User interfaces for continuum robot arms," in *IEEE/RSJ International Conference on Intelligent Robots and Systems*, 2005, pp. 3123–3130.

[11] M. D. Grissom, V. Chitrakaran, D. Dienno, M. Csencits, M. Pritts, B. Jones, W. McMahan, D. Dawson, C. Rahn, and I. Walker, "Design and experimental testing of the octarm soft robot manipulator," in *Unmanned Systems Technology VIII*, vol. 6230. International Society for Optics and Photonics, 2006, p. 62301F.

[12] A. Majewicz and A. M. Okamura, "Cartesian and joint space teleoperation for nonholonomic steerable needles," in *World Haptics Conference (WHC)*, 2013, pp. 395–400.

[13] C. G. Frazelle, A. D. Kapadia, K. E. Fry, and I. D. Walker, "Teleoperation mappings from rigid link robots to their extensible continuum counterparts," in *IEEE International Conference on Robotics and Automation (ICRA)*, 2016, pp. 4093–4100.

[14] H. El-Hussieny, U. Mehmood, Z. Mehdi, S.-G. Jeong, M. Usman, E. W. Hawkes, A. M. Okamura, and J.-H. Ryu, "Development and evaluation of an intuitive flexible interface for teleoperating soft growing robots," in *IEEE/RSJ International Conference on Intelligent Robots and Systems (IROS)*, 2018, pp. 4995–5002.

[15] J. Luong, P. Glick, A. Ong, M. S. deVries, S. Sandin, E. W. Hawkes, and M. T. Tolley, "Eversion and retraction of a soft robot towards the exploration of coral reefs," in *IEEE International Conference on Soft Robotics (RoboSoft)*, 2019, pp. 801–807.

[16] R. J. Webster III and B. A. Jones, "Design and kinematic modeling of constant curvature continuum robots: A review," *The International Journal of Robotics Research*, vol. 29, no. 13, pp. 1661–1683, 2010.

[17] S. G. Hart and L. E. Staveland, "Development of nasa-tlx (task load index): Results of empirical and theoretical research," in *Advances in psychology*. Elsevier, 1988, vol. 52, pp. 139–183.

[18] F. Ilievski, A. D. Mazzeo, R. F. Shepherd, X. Chen, and G. M. Whitesides, "Soft robotics for chemists," *Angewandte Chemie International Edition*, vol. 50, no. 8, pp. 1890–1895, 2011.

[19] J. M. Walker, N. Zemiti, P. Poignet, and A. M. Okamura, "Holdable haptic device for 4-dof motion guidance," in *IEEE World Haptics Conference (WHC), in press*, 2019.

[20] F. Stroppa, C. Loconsole, S. Marcheschi, N. Mastronicola, and A. Frisoli, "An improved adaptive robotic assistance methodology for upper-limb rehabilitation," in *International Conference on Human Haptic Sensing and Touch Enabled Computer Applications*. Springer, 2018, pp. 513–525.